Green Recovery of Gold through Biosorption, Biocrystallization, and Pyro-Crystallization

ARTICLE *in* INDUSTRIAL & ENGINEERING CHEMISTRY RESEARCH · AUGUST 2010

Impact Factor: 2.59 · DOI: 10.1021/ie100104j

5 AUTHORS, INCLUDING:

Sathishkumar M.
National University of Singapore
78 PUBLICATIONS **2,013** CITATIONS
SEE PROFILE

Vijayaraghavan Kuppusamy
Indian Institute of Technology Madras
102 PUBLICATIONS **3,604** CITATIONS
SEE PROFILE

Shruti Pavagadhi
National University of Singapore
23 PUBLICATIONS **225** CITATIONS
SEE PROFILE

Rajasekhar Balasubramanian
National University of Singapore
235 PUBLICATIONS **3,347** CITATIONS
SEE PROFILE

Green Recovery of Gold through Biosorption, Biocrystallization, and Pyro-Crystallization

M. Sathishkumar,[†] A. Mahadevan,[†] K. Vijayaraghavan,[†] S. Pavagadhi,[†,‡] and R. Balasubramanian*[,†,‡]

Singapore-Delft Water Alliance and Division of Environmental Science and Engineering, National University of Singapore, Singapore 117576, Singapore

Gold recovery from dilute solutions has always been a subject of great interest due to ever increasing demand of this precious metal. In the present study, an attempt had been made to recover this noble metal in ionic, nanocrystalline, and metallic form using a combination of biosorption, biocrystallization, and pyro-crystallization techniques with *Sargassum* biomass as biomaterial. Optimization of process parameters revealed that the biosorption capacity increased with a decrease in pH due to an ion-pairing effect. Kinetic studies showed that the biosorption of Au(III) onto *Sargassum* biomass was a rapid process with more than 90% removal at the initial 15 min. Nonlinear forms of pseudofirst-order and pseudosecond-order models were used to fit the experimental data. The adsorption capacity (Q_{max}) from the Langmuir model was found to be 32.94 mg/g at pH 2. Maximum desorption of 97.8% was achieved with 2 N NaOH used as desorption medium. Biocrystallization of ionic gold through bioreduction was observed from 30 min with high productivity at pH 8. The X-ray diffraction analysis (XRD) patterns of the gold nanoparticles revealed their biphasic nature. Recovery of the biosorbed ionic gold in metallic form through pyro-crystallization technique showed the possibility of 91.44% recovery of the metal in pure form as revealed by XRD analysis. The overall results indicate that gold from dilute solutions can be recovered through green processes in ionic, nanocrystalline, or metallic form as desired by the end-consumer using *Sargassum* biomass as biomaterial.

Introduction

Precious metal recovery from dilute solutions remains a subject of great interest from both fundamental and applied research viewpoints.[1] Among precious metals, gold holds a prominent place as it determines the wealth of a nation. Moreover, there are several new and emerging applications, electronics, catalysts, and medical instruments.[2] From these sources, gold and many other precious metals get into the industrial effluent streams in dilute concentrations.[2] Gold is generally recovered from dilute solution by precipitation with zinc powder, sorption by activated charcoal, or solvent exchange.[1–3] An alternative to these methods has recently been proposed on the basis of the use of ionic exchange resins. However, the use of resins has drawbacks such as low selectivity for gold, low efficiency in dilute solution, and high cost.[3] Application of other techniques such as thermal evaporation and precipitation is often very expensive or less efficient for dilute solutions.

Biosorption is a promising alternative for the removal of metal ions from contaminated effluents based on the ability of certain biological materials to concentrate organic or inorganic substances in solution. Quite a number of intensified research studies on biosorption of metal ions have been done in the past two decades.[1–7] A wide range of biomaterials such as bacteria, fungi, algae, yeast, and plant biomass and metabolites such as extracellular polysaccharides have been studied for their potential to biosorb various metals and organic pollutants.[4–7] Nonliving organisms or waste from manufacturing processes involving these organisms can be used as substrates for the sorption of metals from solution. In comparison with synthetic resins, these biomasses are relatively cheap and available in large quantities worldwide. The most promising biosorbents for adsorptive removal of gold are derived from macroalgae and microorganisms whose cell walls include polysaccharides with functional groups such as carboxylates, sulfates, phosphates, and amino-polysaccharides that are responsible for ionic adsorption.[8]

The use of biocrystallization for recovery of metals, especially precious metals using biomaterials, has been explored by a number of researchers in recent years .[9–13] The chemicals or enzymes present in these biomaterials act as reducing agents and crystallize the metals in ionic form to zerovalent metal form. The resultant crystals usually occur as nanosized particles. This nonsynthetic route has an added advantage since precious metals in nanosized particles are more valuable as they find their applications in fields ranging from electrochemistry to medicine.

Pyro-crystallization of precious metals is an age old technique used to recover gold from low-grade ores and wastewaters.[1] This technique uses high temperature for crystallizing the gold. This process is an easily applicable technique, but for industrial effluents containing target metals in trace quantities, its economic feasibility is very low as it requires high energy consumption.

In the present study, we have explored the use of dried biomass of *Sargassum* sp. as a biomaterial for recovery of gold in various forms from the aqueous phase. For this purpose, we employed the biosorption and biocrystallization techniques following the bioreduction of ionic gold to its zerovalent form (gold nanoparticles). In addition, we also studied the possibility of gold recovery in the metallic/crystalline form from the biosorbent through pyro-crystallization. The overall aim of the study was to develop effective green techniques to recover gold

* To whom correspondence should be addressed. E-mail: eserbala@nus.edu.sg.
[†] Singapore-Delft Water Alliance.
[‡] Division of Environmental Science and Engineering.

10.1021/ie100104j
Published on Web 07/01/2010

from the aqueous phase in various forms for potential industrial applications.

Materials and Methods

Preparation of Biomaterial and Gold Solution. *Sargassum* sp. was collected from local beaches of Singapore, washed thoroughly to remove adhering sand particles and other impurities, and dried under sunlight for a week to completely remove the moisture. The algal biomass was then powdered in a mixer and then sieved using a 20-mesh sieve to get a uniform size range. The final sieved powder was used for all further studies.

A 1000 mg/L gold(III) stock solution was prepared using $HAuCl_4 \cdot 3H_2O$. Working standards were prepared from the stock solution according to the required concentrations. NaOH and HCl (0.1 M) were used for pH adjustment. All reagents, unless otherwise indicated, were AnalaR grade purchased from Sigma-Aldrich.

Biosorption Studies. Metal uptake studies were conducted at room temperature and involved contacting 10 mL of $HAuCl_4$ solution with 10 mg of biomass for predetermined intervals on an orbital shaker at 150 rpm. All studies were carried out in duplicate and biomass-free controls were run concurrently. The flasks were withdrawn at predetermined time intervals. The adsorbent was removed by centrifugation at 7500 rpm for 10 min, and the Au concentration of the supernatant was analyzed in inductively coupled plasma-atomic emission spectrometry (ICP-AES; Perkin-Elmer Optima 3000DV). The amount of Au adsorbed by the biomass (q, mg/g) was calculated. The optimal pH for Au removal by the biosorbent was determined by measuring uptake from 10 mL of 100 mg/L Au solutions over a range of pH values from 2 to 10. The solution pH was adjusted using 1 M HCl and 1 M NaOH. Adsorption isotherm experiments were carried out with a series of solutions of initial Au concentration ranging from 10 to 100 mg/L at the optimal pH value determined as described above. Kinetic experiments were conducted in the same manner described above, but the samples were collected at different time intervals to determine the time at which biosorption equilibrium has been attained. The amount of Au sorbed by the biosorbent was calculated from the differences between the concentrations of Au added to those detected in the supernatants, using the following equation:

$$Q = V(C_0 - C_f)/M \tag{1}$$

where Q is Au uptake (mg/g), C_0 and C_f are the initial and equilibrium Au concentrations in the solution (mg/L), respectively, V is the solution volume (L), and M is the mass of biosorbent (g). The data modeling was performed by nonlinear regression using the Sigma Plot (version 4.0, SPSS, USA) software.

The average percentage error between the experimental and predicted values was calculated using

$$\varepsilon(\%) = \frac{\sum_{i=1}^{N} (Q_{exp,i} - Q_{cal,i}/Q_{exp,i})}{N} \times 100 \tag{2}$$

where Q_{exp} and Q_{cal} represent the experimental and calculated uptake values, respectively, and N is the number of measurements.

The residual root-mean-square error (RMSE) was also used to measure the goodness-of-fit between the experimental and predicted values. RMSE can be defined as

$$\mathrm{RMSE} = \sqrt{\frac{1}{m-2}\sum_{i=1}^{m}(Q_i - q_i)^2} \tag{3}$$

where Q_i is the observation from the batch experiment, q_i is the estimate from the isotherm for corresponding to Q_i, and m is the number of observations in the experimental isotherm. The smaller RMSE value indicates the better curve fitting.

Desorption studies were carried out with adsorbate-laden adsorbent obtained from a batch process, in which the adsorbate solutions (50 mg/L of Au) were treated for the optimum contact time. The Au-laden adsorbent was washed gently with distilled water to remove unadsorbed Au. Several such samples were prepared. Then, the spent adsorbent was agitated at 200 rpm for 5 h with 50 mL of distilled water, adjusted to different pH values (2−10). The desorbed Au was estimated spectrophotometrically as mentioned earlier. Similarly, desorption studies were carried out in 50 mL of 2 N NaOH solution, 70% ethanol, 70% acetone, and distilled water separately. The flasks were agitated at 200 rpm for equilibrium time. All the experiments were carried out in duplicate, and the mean values are presented. The error obtained was ±4%.

$$\text{desorption efficiency}\,(\%) = \frac{\text{desorbed Au(III)}\,(\text{mg})}{\text{initially sorbed of Au(III)}\,(\text{mg})} \times 100 \tag{4}$$

Bioreduction and Biocrystallization. For crystallization of gold ions through bioreduction, 50 mg of dry powder of *Sargassum* sp. was carefully weighed and added to 10 mL of 1000 mg/L aqueous $HAuCl_4$ solution in a 50 mL Falcon tube. The flasks were then incubated in a rotary shaker at 160 rpm at room temperature. The rate of bioreduction was monitored for predetermined intervals over a period of 72 h in a UV−vis spectrophotometer (Hitachi, U2800, Japan). For the analysis, 0.1 mL of the sample was taken in a cuvette and was diluted to 2 mL with deionized water. The UV−visible spectra of the resulting diluents were monitored as a function of reaction time at a resolution of 1 nm. After the reaction of 72 h, the reaction mixture was kept aside without any disturbance for 5 min. By then, the biomass had settled at the bottom of the Falcon tubes, and the suspension above was sampled for field emission scanning electron microscopy (FESEM) observation. FESEM observations were performed on a JEOL JSM-6700F instrument (Japan). Energy dispersive X-ray (EDX) analyses were performed on a JEOL JSM-6400 microscope (Japan) fitted with an Oxford-6506 (England) EDX analyzer. Crystallinity of the samples was analyzed through X-ray diffraction analysis (Shimadzu LabX-XRD 6000).

Pyro-Crystallization. After sorption, the gold-loaded sorbent was incinerated in an electric furnace (Carbolite-1100, USA) at 1100 °C for 2 h, and the resultant ash was weighed. The gold-loaded sorbent and the porcelain boat were weighted before the burning experiment. After the incineration was completed, the boat was removed from the furnace and allowed to cool down at room temperature. The weight of the ash was calculated by subtracting the weight of the boat from the total weight. Then, 10 mL of aqua regia (3:1 HCl and HNO_3) was added, and the solution was stirred for 6 h to dissolve gold. The concentration of gold in this aqueous solution was then analyzed by ICP. The crude ash generation and recovery efficiency of gold were calculated from ICP-AES analysis using the follow equations:

$$\text{crude ash generation}(\%) = \frac{\text{weight of ash (mg)}}{\text{weight of metal loaded sorbent (mg)}} \times 100 \quad (5)$$

$$\text{recovery efficiency}(\%) = \frac{\text{weight of metal in ash (mg)}}{\text{weight of initially sorbed metal (mg)}} \times 100 \quad (6)$$

Results and Discussion

Biosorption Studies. Effect of pH. pH is one of the most important parameters that affects the speciation of metals in solution through hydrolysis, complexation, and redox reactions during metal recovery.[14] In the present study, the effect of pH on the gold uptake with *Sargassum* from $AuCl_4^-$ solutions was studied in the pH range of 2−10. A decrease in pH resulted in an increase in the percent uptake of $AuCl_4^-$ ions (Figure 1A). A maximum adsorption was observed at pH 2. Feng et al.[15] reported a similar trend for biosorption of Au(III) by *Rhodobacter capsulatus*. High biosorption of tetrachloroaurate ions in acidic pH was believed to be due to the protonation of functional groups such as amine groups on the algal surface. The adsorption between negatively charged tetrachloroaurate ions and positively charged groups like amines on algal biomass is mainly due to an ion-pairing mechanism. In general, brown algae are reported to be a very good adsorbent for anions including $AuCl_4^-$.[16–18] *Sargassum* biomass was reported to be very rich in amine groups.[17] In addition, lower pH leads to higher concentrations of protons, which neutralizes the overall negative charges of *Sargassum* biomass, makes binding groups carry more positive charges at low pH, and strengthens $AuCl_4^-$ biosorption by means of electrostatic attractions and ion pairing.[15] On the other hand, Feng et al.[15] described that the reason for high adsorption at lower pH might be that $AuCl_4$ has a lower solubility and is, thus, more adsorbable at a lower pH.

Effects of Contact Time. The sorption kinetics plays a very important role in the treatment of contaminated effluents, as it provides valuable insights into the reaction pathways and mechanisms of sorption reactions. The experiments were carried out at a fixed adsorbent dose (100 mg) with 100 mg/L of $AuCl_4^-$ initial concentrations for different time intervals at pH 2 and 30 °C. Since biosorption is a metabolism-independent process, it would be expected to be a very fast reaction. Experimental kinetic data at different initial $AuCl_4^-$ concentrations concurred with this expectation, with around 90% of $AuCl_4^-$ removed in the initial 15 min (Figure 1B). This initial quick phase was followed by slow attainment of equilibrium. After 25 min, no major difference in percent uptake of $AuCl_4^-$ ions were noticed. Song et al.[19] reported around 150 min as equilibrium time for biosorption of Au(III) by *Stenotrophomonas* sp., whereas Moore et al.[20] reported around 72 h for complete removal of gold ions by a fungal strain with an initial concentration of 50 mg/L. *Rhodobacter capsulatus* showed an equilibrium time of 30 min for Au(III) biosorption.[15] Equilibrium time reported for the above-mentioned biomaterials to adsorb Au(III) was much higher as compared to *Sargassam* biomass used in the present study, which highlights the potential use of the latter biomaterial in an industrial scale. Equilibrium time is one of the important considerations in the design of industrial effluent treatment systems because it influences the size of the reactor, thereby the plant economics.[21]

It was also perceived that for an initial $AuCl_4^-$ concentration of 100 mg/L, the maximum amount of $AuCl_4^-$ adsorbed by *Sargassum* biomass for the first 3 and 6 min was at an average adsorption rate of 8.13 and 6.63 mg per g per min, respectively.

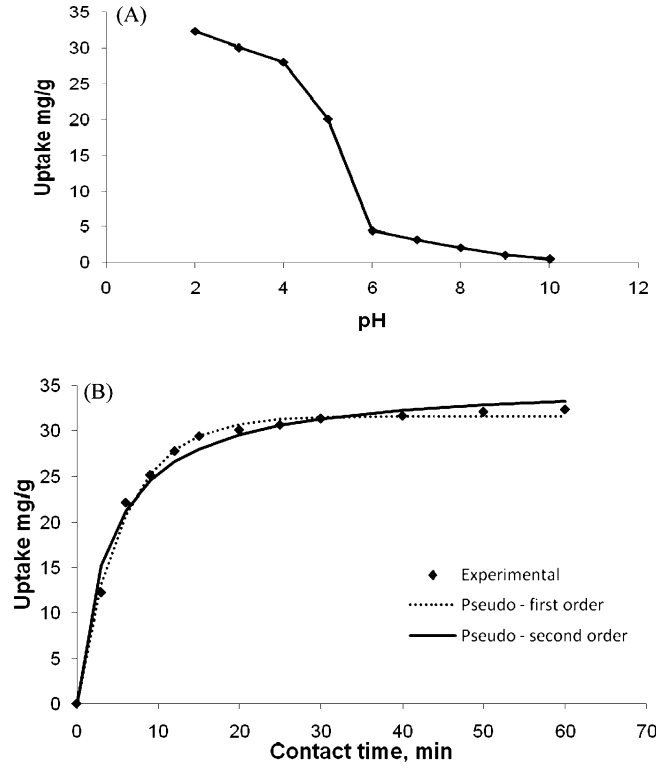

Figure 1. Effect of pH (A) and contact time (B) on biosorption of gold by *Sargassum* biomass.

For the next 9, 12, and 15 min, it was observed to be at 1.97, 1.77, and 1.1 mg per g per min, and thereafter, the adsorption rate tended to decline and proceed at an average adsorption rate of 0.13 mg per g per min until 60 min. This observation elucidates that the uptake of $AuCl_4^-$ ions by *Sargassum* biomass is a very rapid process, where the majority of the uptake was over within the initial 6 min and it then gradually decreased to attain equilibrium. The initial rapid phase is thought to be due to the abundant availability of adsorption/vacant sites on the biomass which in turn facilitated easy diffusion of Au(III) ions into the pores of the particles. This physical process resulted in an increased concentration gradient between the adsorbate in solution and that in the adsorbent.[22] Asfour et al.[23] explained that this fast sorption process might be due to strong attractive forces between the sorbate molecules and the sorbent, leading to fast diffusion into the intraparticle matrix to attain rapid equilibrium.

Kinetic Modeling. Pseudofirst- and pseudosecond-order models were used to describe the experimental kinetic data. Application of both models resulted in very high correlation coefficients and low % error and RMSE values. However, the pseudofirst-order model predicted the equilibrium uptake values and kinetic curves better compared to the pseudosecond-order model. The equilibrium uptake values predicted by pseudofirst- and pseudosecond-order models were 31.64 and 35.54 mg/g, compared to the experimental equilibrium uptake of 32.35 mg/g. On the basis of the error analysis, data predicted by the pseudofirst-order model ($R^2 = 0.999$; ε (%) = 2.2; RMSE = 0.508) deviated less than that by the pseudosecond-order model ($R^2 = 0.997$; ε (%) = 2.9; RMSE = 0.9) compared to the experimental data. The pseudofirst- and pseudosecond-order rate constants were 0.178 and 0.007, respectively. The curves predicted by the pseudofirst- and pseudosecond-order models are shown in Figure 1B, which also shows that the curves predicted by the pseudofirst-order model coincided well with

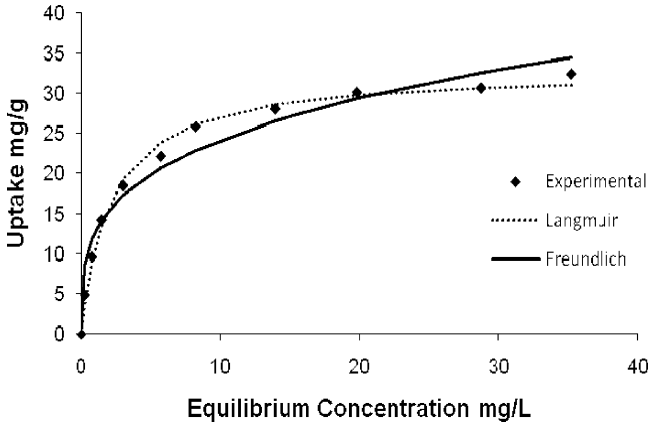

Figure 2. Biosorption isotherm at pH 2.

experimental data with high correlation coefficient and low % error values.

Isotherm Modeling. Isotherms pertaining to the sorption of $AuCl_4^-$ onto *Sargassam* biomass were determined at different initial $AuCl_4^-$ concentrations ranging from 10−100 mg/L (Figure 2). A critical analysis of the shape of isotherms revealed that the isotherm was favorable and can be classified as "L-shaped".[24] This means the ratio between the $AuCl_4^-$ concentration in the solution and that sorbed onto the biosorbent decreases with an increase in the $AuCl_4^-$ concentration, providing a concave curve without a plateau. The Langmuir model served to estimate the maximum $AuCl_4^-$ uptake values which could not be reached in experiments. The constant b_L represents affinity between the adsorbent and adsorbate. Initially, the Langmuir model was applied to the present system, with the assumptions that adsorption sites are identical, each site retaining one molecule of the given compound, and all sites are energetically and sterically independent of the adsorbed quantity. Even though these assumptions are not valid for a biomaterial used as sorbent, the model was able to describe the isotherm data with high R^2 and low % error values ($R^2 = 0.999$; ε (%) = 4.15; RMSE = 1.81). A maximum $AuCl_4^-$ biosorption capacity of 32.94 mg/g was observed. High values of b_L (0.49) are reflected in the steep initial slope of a sorption isotherm, indicating desirable high affinity. Thus, for good biosorbents in general, high Q_{max} and a steep initial isotherm slope (i.e., high b_L) are desirable. The Freundlich model also showed a reasonably good fit with high R^2 and low % error values ($R^2 = 0.999$; ε (%) = 6.24; RMSE = 4.09). However, the curve predicted by this model significantly deviated from the experimental data compared to the Langmuir isotherm (Figure 2). The Freundlich isotherm was originally empirical in nature but was later interpreted as sorption to heterogeneous surfaces or surfaces supporting sites of varied affinities. It is assumed that the stronger binding sites are occupied first and that the binding strength decreases with the increasing degree of site occupation. High K_F and $1/n$ values ($K_F = 12.69$;$1/n = 3.6$) indicate that the binding capacity reached its highest value, and the affinity between the biosorbent and $AuCl_4^-$ was also high.

Desorption. Regeneration and reuse of the adsorbent is a very important issue to be addressed when applied industrially. Desorption was attempted in ethanol, methanol, acetone, and strong alkali (2 N NaOH). Desorption was also attempted in deionized water for comparison. The sorbate-laden *Sargassum* biomass (50 mg) was suspended in 10 mL of the above-mentioned desorbing media and agitated in a rotary shaker at 150 rpm for 8 h. Acetone, ethanol, methanol, NaOH, and water showed 8.6, 31.6, 38.5, 97.8 and 0.6% desorption, respectively.

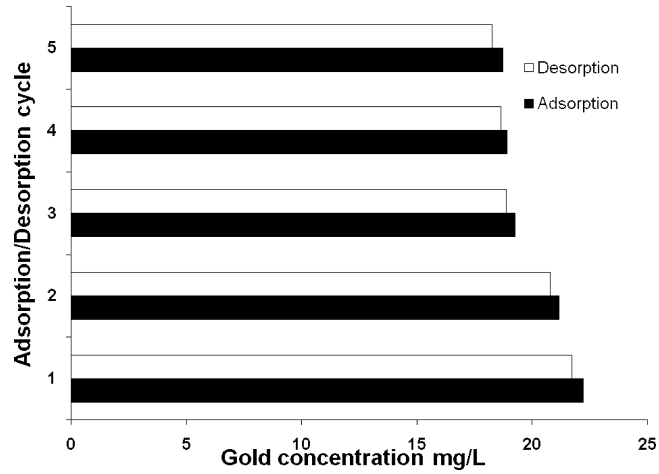

Figure 3. Adsorption/desorption efficiency at repeated cycles.

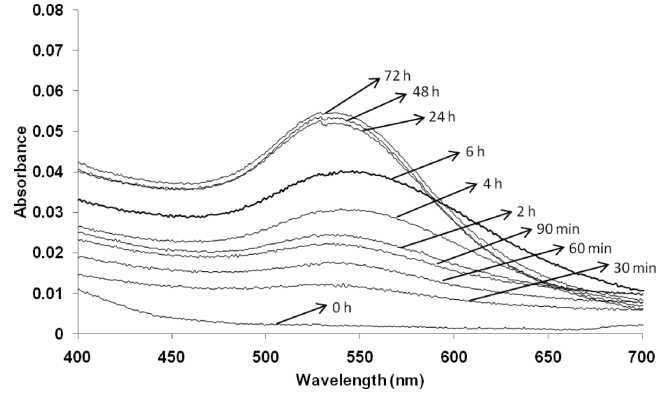

Figure 4. UV−visible spectra recorded as function of time.

Adsorption/desorption was repeated using NaOH as desorption medium for five consecutive cycles to examine the possibility of reusing the biosorbent (Figure 3). Comparing the difference in adsorption between the first and fifth cycles showed a 15% decrease in the adsorption efficiency. This reduction could be attributed to the loss of surface functional groups which in turn could be due to cell damage caused by strong alkali which was used as desorption medium. However, the recovery of gold after each desorption cycle was almost 98%.Thus, the adsorbent can be reused for several cycles until the rigidity of the biomass is still suitable for adsorption. Since the biomass is easily biodegradable, it can be dumped "as is" or can be subjected to composting after several cycles of adsorption as explained by Binupriya et al.[25]

Biocrystallization through Bioreduction. The *Sargassum* biomass−$HAuCl_4$ reaction mixture showed a visible color change from colorless/straw color to reddish purple after 30 min of reaction, which was quite evident for gold nanoparticle formation.[12,26–28] The color of the solution remained unaltered even after 3 months without settling. The formation and stability of the reduced gold nanoparticles in the colloidal solution was monitored using UV−vis spectral analysis. An UV−vis spectrum is one of the important techniques that can be used to ascertain the formation of metal nanoparticles, provided surface plasmon resonance exists for the metal. Figure 4 shows that an increase in time increased the intensity of the peak, but after 24 h, the increase in the intensity is very meagre, which may be due to the saturation of the reaction. The most interesting observation here was the rapid bioreduction of gold ions to crystalline form. Even by 30 min, the peak was observed, which represents the nanoparticle formation, and by 360 min, the

intensity of the peak increased more than 3-fold. Synthesis of nanoparticles through bioroute is generally considered to be impractical due to the time taken for reduction process. Binupriya et al.[12] reported more than 3 days for saturation of the reaction process for biocrystallization of gold by *Aspergillus oryzae*. Similarly, Govindaraju et al.[28] and Singaravelu et al.[27] reported more than 12 and 1 h, respectively, for initiation of nanoparticle synthesis process. It was observed from the spectra that the gold surface plasmon resonance band occurs at about 540 nm,[29] and this absorption steadily increased in intensity as function of time of reaction. The interaction of light having a wavelength smaller than the particle size of Au NPs leads to polarization of the free conduction electrons with respect to the much heavier ionic core of Au NPs. Therefore, an electron dipolar oscillation is created, and a surface plasmon (SP) absorption band is obtained.[30] SP resonance studies of Au NPs at various pH clearly indicate the formation of Au NPs at pH 8 is higher. In acidic pH, the formation was almost negligible. This observation shows that acidic pH is not favorable for Au NP production. Agnihotri et al.[31] reported a similar result for production of Au NPs by marine yeast, *Yarrowia lipolytica*, in which case acidic pH did not favor Au NP synthesis much, but a greater number of larger-sized crystalline gold triangles and hexagons than near-spherical particles were observed compared to other pH values. He et al.[32] reported a similar result for Au NPs synthesis by *Rhodopseudomonas capsulata* at lower pH. Binupriya et al.[12] reported that at higher pH the particles were mostly spherical and were smaller in size compared to that at acidic pH values. Studying the final pH values of the reaction mixtures after the bioreduction/biocrystallization process showed a sharp decrease in pH values in the pH range between 5 and 10, which is a clear evidence for gold reduction, whereas in acidic pH not much variation in final pH was noticed. Mata et al.[18] and Sathishkumar et al.[9] reported an analogous result for reduction of gold and silver by *Fucus vesiculosus* and *Cinnamon zeylanicum*, respectively. A decrease in pH on gold reduction may be due to release of protons as described in the following equation.[33]

$$AuCl_4^- + 3R{-}OH \rightarrow Au^0 + 3R{=}O + 3H^+ + 4Cl^- \quad (7)$$

Kuyucak and Volesky[33] explained that reduction of Au(III) to Au(0) occurs through oxidation of hydroxyl to carbonyl groups (C−OH to C═O). Algal cell walls are abundant in polysaccharides containing hydroxyl groups.[17] Polyphenols are another class of natural compounds majorly responsible for metal reduction.[9,34,35] *Sargassum* is also reported to be rich in these polyphenols. In addition, *Sargassum* is known to contain a class of polyphenolic compounds known as Pholorotannins. Like other polyphenolic compounds, these are also produced from plant metabolism.[36] These compounds are characteristic for brown algae. Phlorotannins play a primary role in acting as integral structural components of cell walls. They are suggested to act as other phenolic compounds and to behave as strong antioxidant agents.[37,38] Shankar et al.[29] deduced that the reduction of the metal ions is possibly facilitated by reducing sugars and/or terpenoids present in the neem leaf broth while Singaravelu et al.[27] contributed the stabilization of nanoparticles to the presence of extracellular polysaccharides in seaweed *Sargassum wightii*.

Field emission scanning electron microscopy (FESEM) analysis was carried out after 72 h of reaction. Precisely scattered nanoparticles with sporadic aggregation were seen both on the surface of the biomaterial and in the aqueous phase. This spectral analysis shows that the gold ions are first adsorbed on the algal

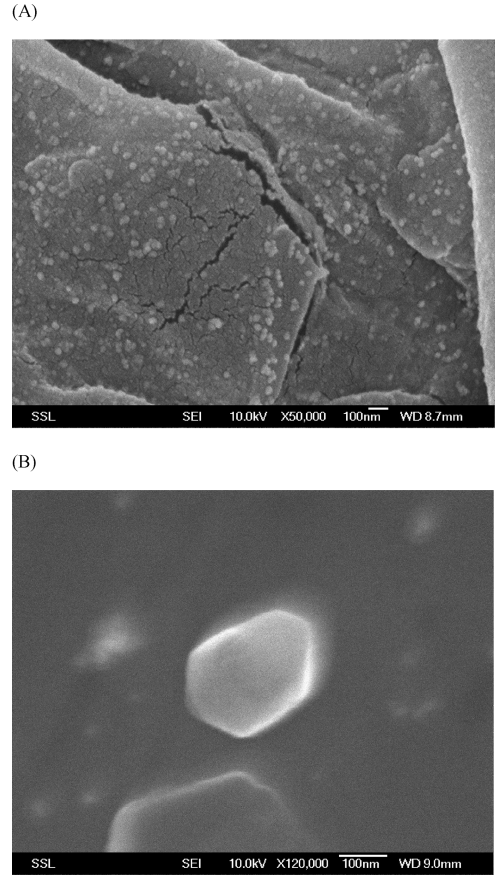

Figure 5. FESEM image of gold nanoparticles on the surface of *Sargassum* biomass (A) and the extracellular aqueous phase (B).

biomass by an electrostatic attraction/ion-exchange mechanism and later reduced by either enzymes or organics present in the biomaterial. In the case of nanoparticles in the aqueous phase, the organics leached out of the biomaterial would have reduced the gold ions to crystalline form and some nanoparticles could have been detached from the biomaterial surface due to shaking. Algal cells are known to adsorb the cationic and anionic metal ions on their cell surface through functional groups.[16−18,33] On the surface of the biomaterial, gold nanoparticles ranging from 20 to 80 nm were observed devoid of any triangular or hexagonal nanoplates (Figure 5A). However, in the aqueous phase, in addition to near-shperical particles, triangular or hexagonal nanoplates around 100−200 nm in size were seen (Figure 5B). These results are comparable to the results reported by Liu et al.[39] However, the phenomenon behind the formation of nanoparticles with specific shapes and geometries is still unclear, and further research is needed. Liu et al.[39] explained this phenomenon with the following hypothesis: As per the assumption, the biomaterial provided both the reducing agent(s) and the capping agents (A and B) necessary for the gold nanoplate synthesis from its range of functional biochemicals. The capping agents may be further divided into two classes. One assisted to limit the size (A) and the other assisted to control the shape (B). Hence, A would bind nonspecifically on all exposed surfaces of gold whereas the binding of B was stronger on certain facets of gold. Depending on the availability of A and B on the biomaterial surface or aqueous phase, the shape of the nanoparticles varies.

The particles were further verified using EDX analysis to ensure the presence of Au. The EDX spectrum also showed that 87.6% of the elemental composition was gold. The crystallinity of the prepared nanoparticles was investigated by

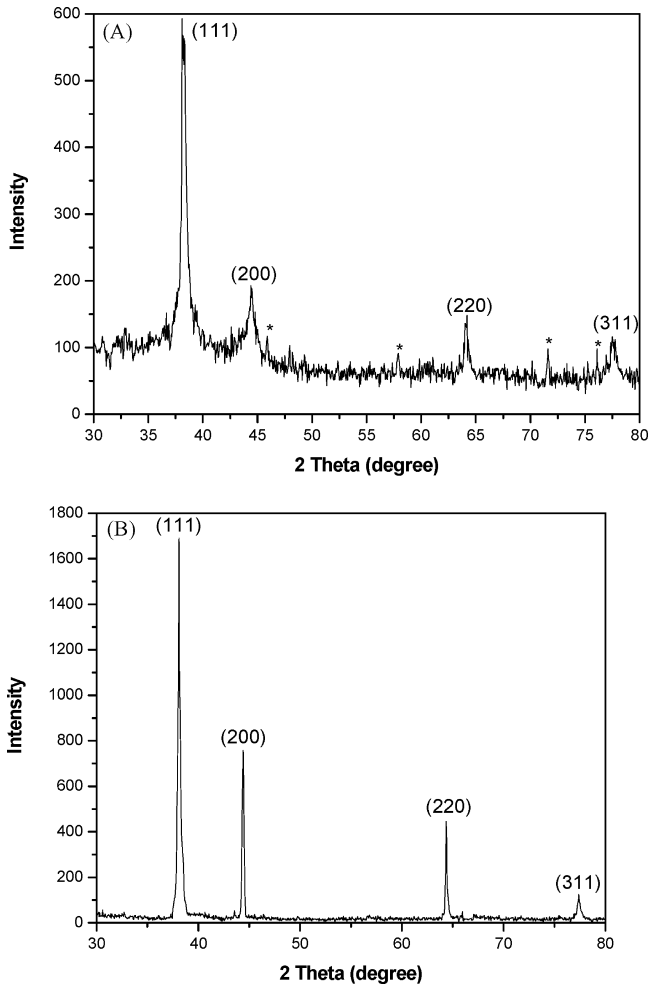

Figure 6. XRD pattern of gold nanoparticles synthesized through biocrystallization (A) and pyro-crystallization (B).

the X-ray diffraction technique and corresponding X-ray diffraction analysis (XRD) patterns are shown in Figure 6A. The synthesized Au NPs have shown clear peaks of cubic phases (JCPDS No. 03-0921) at 38.1 (1 1 1), 44.4 (2 0 0), 64.4 (2 2 0), and 77.5 (3 1 1). In addition, some minor peaks representing the hexagonal phases (JCPD No. 41-1402) at 45.9 (1 0 0), 57.9 (1 0 3), 71.6 (0 0 6), and 76.1 (1 0 5) were also noticed (represented using an asterisk in Figure 6A). It suggests that the gold nanoparticles obtained through biosynthesis are biphasic in nature. The slight shift in the peak positions indicated the presence of a strain in the crystal structure which is a characteristic of nanocrystallites.[9,12] The broad bottom area of the peaks indirectly represents the smaller size of the nanoparticles. Thus, the XRD pattern provides a strong evidence that is complementary to the UV−vis spectra and FESEM images for the presence of gold nanocrystals.[31,40]

Pyro-Crystallization. Pyro(thermal)-crystallization is a conventional technique for recovery of gold from ores after leaching. We applied this technique in the current study for the recovery of gold following the uptake of ionic gold through biosorption. Our intention was to combine biosorption with incineration to recover the gold in metallic form rather than in ionic form through desorption. The incineration of Au(III) loaded *Sargassum* biomass at 1100 °C in a muffle furnace resulted in ash containing the metallic gold. The crude ash generation was found to be 9.47%. The conversion of ionic gold to crystalline form in ash through the incineration technique was confirmed with the X-ray diffraction technique, and the corresponding XRD patterns are shown in Figure 6B. The clear peaks of pure gold at 38.1 (1 1 1), 44.44 (2 0 0), 64.38 (2 2 0), and 77.34 (3 1 1) were observed (JCPDS No. 03-0921). No other noticeable peaks were seen. The peaks were very sharp and narrow, which epitomize the large size of the gold crystals. The metal in ash was dissolved using aqua regia, and the content was measured using ICP-AES as mentioned earlier. The recovery efficiency of gold was calculated from the metal in ash, which was found to be 91.44%. From the high recovery efficiency, it is very apparent that the pyro-crystallization technique employed in the present study to recover biosorbed ionic gold in metallic form is a promising, cost-effective technique for the recovery of gold from *Sargassum* biomass.

Conclusions

From the present study on the recovery of gold in aqueous phase using a combination of biosorption, biocrystallization, and pyro-crystallization techniques, the following major conclusions can be drawn

- Biosorption of Au(III) onto *Sargassum* biomass was pH dependent and was found to increase with a decrease in pH, which could be attributed to an ion-pairing mechanism.
- Adsorption was found to be very rapid with more than 90% Au(III) biosorption at the initial 30 min and maximum adsorption capacity (Q_{max}) of 32.94 mg/g as predicted by Langmuir isotherm.
- 97.8% desorption was achieved with 2 N NaOH as desorption/eluting media.
- Nanoparticle formation was clearly evident from 30 min, and no major difference in productivity was noticed beyond 24 h.
- Higher nanoparticle productivity was observed at pH 8, and lower productivity was observed at acidic pH.
- Incineration of Au(III)-loaded biosorbent resulted in 91.44% recovery of gold in metallic form.

It could, thus, be concluded that *Sargassum* biomass can be used as a potent biomaterial for recovery of liquid-phase gold in ionic, metallic, and nanocrystalline forms. In addition, since *Sargassum* biomass is easily available in large quantities as waste material, its use for gold recovery in a desired form would bring down the process costs significantly and can be viewed as an eco-friendly and effective waste biomaterial management strategy.

Acknowledgment

The authors gratefully acknowledge the support and contributions of this project to the Singapore-Delft Water Alliance (SDWA). The research presented in this work was carried out as part of the Singapore-Delft Water Alliance (SDWA)'s research programme (R-264-001-013-272).

Literature Cited

(1) Won, S. W.; Mao, J.; Kwak, I. S.; Sathishkumar, M.; Yun, Y. S. Platinum Recovery from ICP Wastewater by a Combined Method of Biosorption and Incineration. *Bioresour. Technol.* **2010**, *101*, 1135.

(2) Ramesh, A.; Hasegawa, H.; Sugimoto, W.; Maki, T.; Ueda, K. Adsorption of Gold(III), Platinum(IV) and Palladium(II) onto Glycine Modified Crosslinked Chitosan Resin. *Bioresour. Technol.* **2008**, *99*, 3801.

(3) Torres, E.; Mata, Y. N.; Blazquez, M. L.; Munoz, J. A.; Gonzalez, F.; Ballester, A. Gold and Silver Uptake and Nanoprecipitation on Calcium Alginate Beads. *Langmuir* **2005**, *21*, 7951.

(4) Sathishkumar, M.; Binupriya, A. R.; Swaminathan, K.; Choi, J. G.; Yun, S. E. Bio-Separation of Toxic Arsenate Ions from Dilute Solutions by Native and Pretreated Biomass of *Aspergillus fumigatus* in Batch and

Column Mode: Effect of Biomass Pre-Treatment. *Bull. Environ. Contam. Toxicol.* **2008**, *81*, 316.

(5) Binupriya, A. R.; Sathishkumar, M.; Swaminathan, K.; Ku, C. S.; Yun, S. E. Comparative Studies on Removal of Congo Red by Native and Modified Mycelial Pellets of *Trametes versicolor* in Various Reactor Modes. *Bioresour. Technol.* **2008**, *99*, 1080.

(6) Vijayaraghavan, K.; Mao, J.; Yun, Y. S. Biosorption of Methylene Blue from Aqueous Solution Using Free and Polysulfone-Immobilized *Corynebacterium glutamicum*: Batch and Column Studies. *Bioresour. Technol.* **2008**, *99*, 2864.

(7) Lin, Z.; Wu, J.; Xue, R.; Yang, Y. Spectroscopic Characterization of Au^{3+} Biosorption by Waste Biomass of *Saccharomyces cerevisiae*. *Spectrochim.* **2005**, *61*, 761.

(8) Raize, O.; Argaman, Y.; Yannai, S. Mechanism of biosorption of different heavy metals by brown marine macroalgae. *Biotechnol. Bioeng.* **2004**, *87*, 451.

(9) Sathishkumar, M.; Sneha, K.; Won, S. W.; Cho, C. W.; Kim, S.; Yun, Y. S. Cinnamon zeylanicum Bark Extract and Powder Mediated Green Synthesis of Nano-Crystalline Silver Particles and its Bactericidal Activity. *Colloids Surf., B* **2009**, *73*, 332.

(10) Sathishkumar, M.; Sneha, K.; Kwak, I. S.; Juan, M.; Tripathy, S. J.; Yun, Y. S. Phyto-Crystallization of Palladium Through Reduction Process Using *Cinnamon zeylanicum* Bark Extract. *J. Hazard. Mater.* **2009**, *171*, 400.

(11) Binupriya, A. R.; Sathishkumar, M.; Yun, S. I. Myco-crystallization of Silver Ions to Nanosized Particles by Live and Dead Cell Filtrates of *Aspergillus oryzae* var. *viridis* and Its Bactericidal Activity toward *Staphylococcus aureus* KCCM 12256. *Ind. Eng. Chem. Res.* **2010**, *49*, 852.

(12) Binupriya, A. R.; Sathishkumar, M.; Vijayaraghavan, K.; Yun, S. I. Bioreduction of Trivalent Aurum to Nano-Crystalline Gold Particles by Active and Inactive Cells and Cell Free Extract of *Aspergillus oryzae* var *Viridis*. *J. Hazard. Mater.* **2010**, *177*, 539.

(13) Shankar, S. S.; Rai, A.; Ankamwar, B.; Singh, A.; Ahmad, A.; Sastry, M. Biological Synthesis of Triangular Gold Nanoprisms. *Nat. Mater.* **2004**, *3*, 482.

(14) Esposito, A.; Pagnanelli, F.; Veglio, F. pH-Related Equilibria Models for Biosorption in Single-Metal Systems. *Chem. Eng. Sci.* **2002**, *57*, 307.

(15) Feng, Y.; Yu, Y.; Wang, Y.; Lin, X. Biosorption and Bioreduction of Trivalent Aurum by Photosynthetic Bacteria *Rhodobacter capsulatus*. *Curr. Microbiol.* **2007**, *55*, 402.

(16) Kratochvil, D.; Pimentel, P.; Volesky, B. Removal of Trivalent and Hexavalent Chromium by Seaweed Biosorbent. *Environ. Sci. Technol.* **1998**, *32*, 2693.

(17) Davis, T. A.; Volesky, B.; Mucci, A. A Review of the Biochemistry of Heavy Metal Biosorption by Brown Algae. *Water Res.* **2003**, *37*, 4311.

(18) Mata, Y. N.; Torres, E.; Blázquez, M. L.; Ballester, A.; González, F.; Mu∼noz, J. A. Gold(III) Biosorption and Bioreduction with the Brown Alga *Fucus vesiculosus*. *J. Hazard. Mater* **2009**, *166*, 612.

(19) Song, H. P.; Li, X. G.; Sun, J. S.; Xu, S. M.; Han, X. Application of a Magnetotactic Bacterium, *Stenotrophomonas* sp. to the Removal of Au(III) from Contaminated Wastewater with a Magnetic Separator. *Chemosphere* **2008**, *72*, 616.

(20) Moore, B. A.; Duncan, J. R.; Burgess, J. E. Fungal Bioaccumulation of Copper, Nickel, Gold and Platinum. *Miner. Eng.* **2008**, *21*, 55.

(21) Deepa, K. K.; Sathishkumar, M.; Binupriya, A. R.; Murugesan, G. S.; Swaminathan, K.; Yun, S. E. Sorption of Cr(VI) from Dilute Solutions and Wastewater by Live and Pretreated Biomass of *Aspergillus flavus*. *Chemosphere* **2006**, *62*, 833.

(22) Sathishkumar, M.; Binupriya, A. R.; Kavitha, D.; Yun, S. E. Kinetic and Isothermal Studies on Liquid-Phase Adsorption of 2,4-Dichlorophenol by Palm Pith Carbon. *Bioresour. Technol.* **2007**, *98*, 866.

(23) Asfour, H. M.; Fadali, O. A.; Nassaar, M. M.; EI-Geundi, M. S. Equilibrium Studies on Adsorption of Basic Dyes on Hard Wood. *J. Chem. Technol. Biotechnol.* **1995**, *35*, 21.

(24) Limousin, G.; Gaudet, J. P.; Charletm, L.; Szenknect, S.; Barthes, V.; Krimissa, M. Sorption Isotherms: A Review on Physical Bases, Modeling and Measurement. *Appl. Geochem.* **2007**, *22*, 249.

(25) Binupriya, A. R.; Sathishkumar, M.; Kavitha, D.; Swaminathan, K.; Yun, S. E. Aerated and Rotated Mode Decolorization of a Textile Dye from Aqueous Solution by Native and Modified Mycelial Biomass of *Trametes versicolor*. *J. Chem. Technol. Biotechnol.* **2007**, *82*, 350.

(26) Raghunandan, D.; Basavaraja, S.; Mahesh, B.; Balaji, S.; Manjunath, S. Y.; Venkataraman, A. Biosynthesis of Stable Polyshaped Gold Nanoparticles from Microwave-Exposed Aqueous Extracellular Anti-Malignant Guava (*Psidium guajava*) Leaf Extract. *Nanobiotechnology* **2010**, *5*, 34−44.

(27) Singaravelu, G.; Arockiamary, J. S.; Kumar, V. G.; Govindaraju, K. A Novel Extracellular Synthesis of Monodisperse Gold Nanoparticles Using Marine Alga *Sargassum wightii* Greville. *Colloids Surf., B* **2007**, *57*, 97.

(28) Govindaraju, K.; Basha, S. K.; Kumar, V. G.; Singaravelu, G. Silver, Gold and Bimetallic Nanoparticles Production Using Single-Cell Protein (*Spirulina platensis*) Geitler. *J. Mater. Sci.* **2008**, *43*, 5115.

(29) Shankar, S. S.; Rai, A.; Ahmad, A.; Sastry, M. Rapid Synthesis of Au, Ag, and Bimetallic Au core-Ag Shell Nanoparticles Using Neem (*Azadirachta indica*) Leaf Broth. *J. Colloid Interface Sci.* **2004**, *275*, 496.

(30) Link, S.; El-Sayed, M. A. Shape and Size Dependence of Radiative, Nonradiative, and Photothermal Properties of Gold Nanocrystals. *Int. Rev. Phys. Chem.* **2000**, *19*, 409.

(31) Agnihotri, M.; Joshi, S.; Kumar, A. R.; Zinjarde, S.; Kulkarni, S. Biosynthesis of Gold Nanoparticles by the Tropical Marine Yeast *Yarrowia lipolytica* NCIM 3589. *Mater. Lett.* **2009**, *63*, 1231.

(32) He, S. Y.; Guo, Z. R.; Zhang, Y.; Zhang, S.; Wang, J.; Gu, N. Biosynthesis of Gold Nanoparticles Using the Bacteria *Rhodopseudomonas capsulate*. *Mater. Lett.* **2007**, *61*, 3984.

(33) Kuyucak, N.; Volesky, B. Accumulation of Gold by Algal Biosorbent. *Biorecovery* **1989**, *1*, 189.

(34) Shankar, S. S.; Ahmad, A.; Sastry, M. Geranium Leaf Assisted Biosynthesis of Silver Nanoparticles. *Biotechnol. Prog.* **2003**, *19*, 1627.

(35) Huang, J.; Li, Q.; Sun, D.; Lu, Y.; Su, Y.; Yang, X.; Wang, H.; Wang, Y.; Shao, W.; He, N.; Hong, J.; Chen, C. Biosynthesis of Silver and Gold Nanoparticles by Novel Sundried *Cinnanonum camphora* Leaf. *Nanotechnology* **2007**, *18*, 105104, DOI: 10.1088/0957-4484/18/10/105104.

(36) Koivikko, R.; Loponen, J.; Honkanen, T.; Jormalainen, V. Contents of Soluble, Cell-Wall-Bound and Exuded Phlorotannins in the Brown Alga *Fucus vesiculosus*, with Implications on Their Ecological Functions. *J. Chem. Ecol.* **2005**, *31*, 195.

(37) Lim, S. N.; Cheung, P. C. K.; Ooi, V. E. C.; Ang, P. O. Evaluation of Antioxidative Activity of Extracts from a Brown Seaweed, *Sargassum siliquastrum*. *J. Agric. Food Chem.* **2002**, *50*, 3862.

(38) Yan, X. J.; Li, X. C.; Zhou, C. X.; Fan, X. Prevention of Fish Oil Rancidity by Phlorotannins from *Sargassum kjellmanianum*. *J. Appl. Phycol.* **1996**, *8*, 201.

(39) Liu, B.; Xie, J.; Lee, J. Y.; Ting, Y. P.; Chen, J. P. Optimization of High-Yield Biological Synthesis of Single-Crystalline Gold Nanoparticles. *J. Phys. Chem. B.* **2005**, *109*, 15256.

(40) Narayanan, K. B.; Sakthivel, N. Coriander Leaf Mediated Biosynthesis of Gold Nanoparticles. *Mater. Lett.* **2008**, *62*, 4588.

Received for review January 17, 2010
Revised manuscript received May 24, 2010
Accepted June 19, 2010

IE100104J